Mem. S.A.It. Vol. 83, 92

Memorie della

The Crab Nebula in the infrared: a review

P. Persi

IASF-ROMA/INAF, Via Fosso del Cavaliere 100, 00133 Roma, Italy
e-mail: `paolo.persi@iasf-roma.inaf.it`

Abstract. A review of the Crab Nebula in the infrared including ground based and space observations obtained with the ISO and Spitzer satellites is presented. A brief discussion about the discovered of H_2 jets observed at 2.12 μm in the Crab is also reported.

Key words. Stars: SNR – Stars: pulsar – General: Infrared

1. Introduction

The Crab Nebula is one of the brightest synchrotron source in the Galaxy. It is a prototype of a class of SNRs called plerions, which are powered by a central pulsar. The supernova which produced the Crab Nebula is located in the costellation of Taurus at a distance of about 2 kpc.
Comparing the X-ray, optical and infrared images obtained respectively with Chandra, Hubble Space Telescope and the Spitzer Space telescope (see the composite image of Figure 1), results that the nebula appears most compact in X-rays and largest in the infrared. This can be understood by the fact that ultrahigh-energy X-ray emitting electrons radiate away their energy more quickly than the lower-energy electrons emitting optical and infrared radiation.

One of the main reasons to observe the Crab Nebula in the infrared is to test the hypothesis that part of the interstellar dust does originate from SNe. In fact the infrared (IR) is an ideal spectral region in which to test these theories because dust grains emit strongly in the IR. In addition the comparison of the spectral index derived from IR observations with those obtained in the radio and UV-Opt. spectral regions, is foundamental in understanding the physical mechanisms of emission in the Crab Nebula.

In Sect.2 will be presented a review of the main infrared observations of the Crab Nebula, while in Sect.3 are reported the results of the Spitzer images. Finally in Sect.4 the presence of H_2 knots observed in the filaments of the nebula is discussed.

Send offprint requests to: P. Persi

2. Infrared observations

2.1. Near-Infrared

Near-infrared photometric observations of the Crab Nebula were obtained in the past by different authors (Becklin & Kleinmann 1968), (Grasdalen 1979). From the dereddened spectral energy distribution obtained combining the observed integrated flux densities from 1-5 μm with optical data, a spectral index of α= -0.46 ($f_\nu \propto \nu^\alpha$) was derived (Grasdalen 1979) . This value supports the synchrotron mechanism in the near-IR. In addition, the first image at 2.2 μm obtained by Grasdalen (1979) showed a strict correlation with the visible flux distribution.

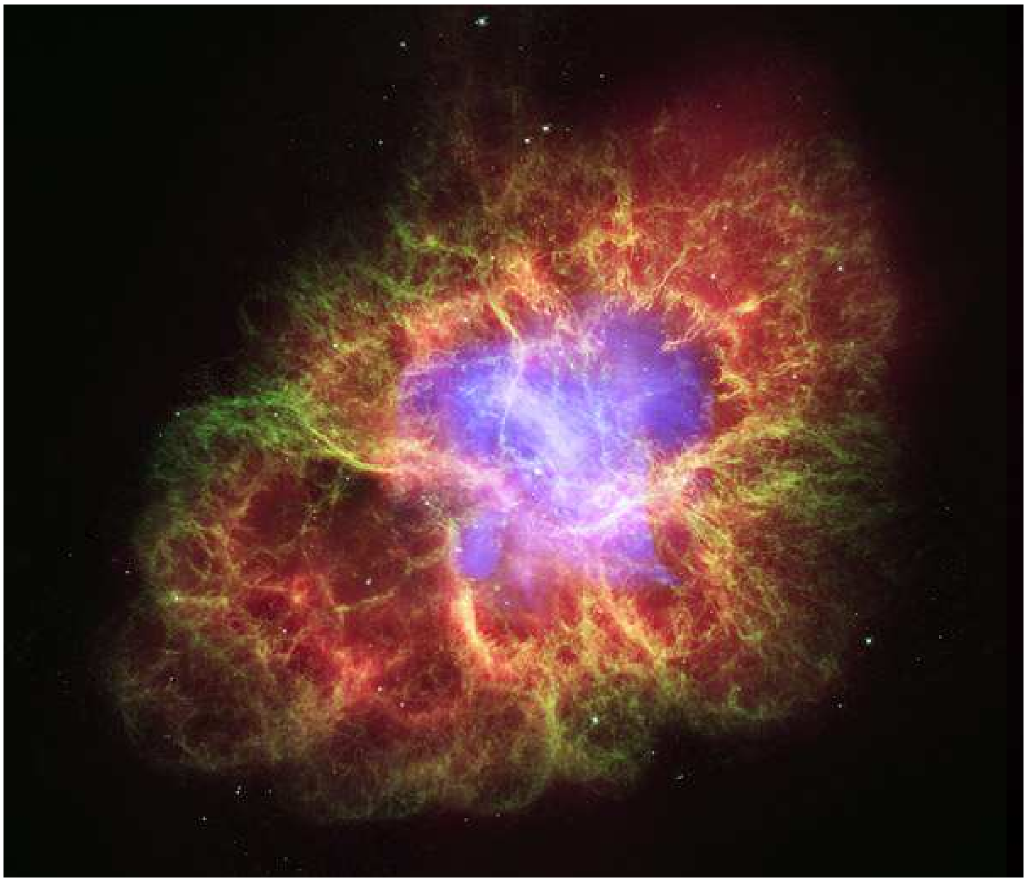

Fig. 1. Composite image of the Crab Nebula obtained with the Chandra X-ray image (blue), Hubble telescope optical image (green), and the Spitzer infrared image (red). Credit: X-ray: NASA/CXC/ASU/J.Hester et al.; Optical: NASA/ESA/ASU/J.Hester and A.Loll; Infrared: NASA/JPL-Caltech/Univ. Minn./R.Gehrz

With the advent of the near-IR array detectors has been possible to study in details the morphology of the nebula and the central pulsar. Particularly interesting are the 1.644 μm images centered on the [Fe II] line obtained by Herster et al. (1990) and Temim et al. (2006) (see Figure 2). These images are dominated by a prominent filament structure identical to the [Ni II] image indicating that the gas phase distribution of Fe^{+} and Ni^{+} are very similar.
Sub-arcsec resolution image in the continuum at 2.2 μm obtained by Melatos et al. (2005) shows the presence of bright and faint equatorial wisps and a polar knot (Figure 3) around the central pulsar. These features appear to fluctuate in brightness on kilosecond timescales.

2.2. Mid and Far-infrared

The Crab Nebula was observed for the first time between 12 and 100 μm with the IRAS satellite (Marsden et al. 1984). The observations show an infrared excess beyond 12 μm over the extraplolated radio and near-IR fluxes peaking between 60 and 100 μm (Figure 4). This has been interpreted as due to thermal radiation by dust at temperature of 46 K and with mass of 0.02 M_{sun} (Strom & Greidanus 1992) . Images at 60 and 100 μm taken with

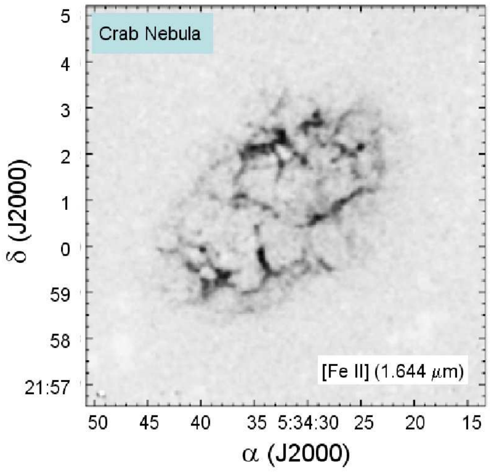

Fig. 2. [Fe II] 1.644 μm image of the Crab Nebula after Temim et al. (2006).

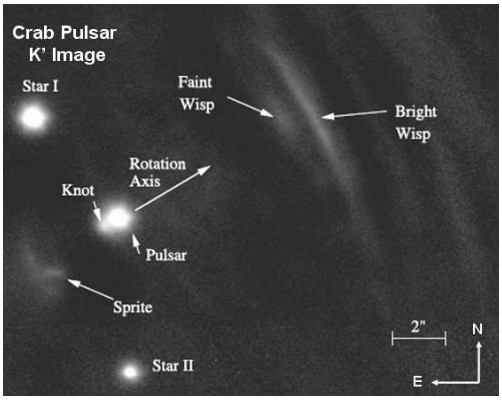

Fig. 3. Sub-arcsec K' image of the central 20 arcsec×20 arcsec region of the Crab pulsar after Melatos et al. (2005). The principal features of the pulsar wind termination shock and its environment are labeled.

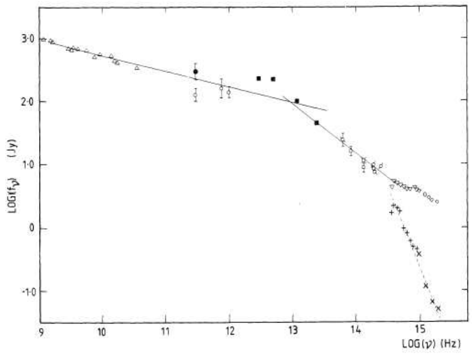

Fig. 4. Spectral energy distribution of the Crab Nebula from UV to radio spectral region after Marsden et al. (1984).

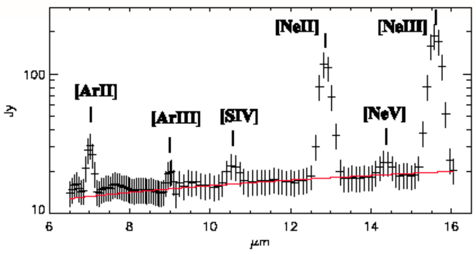

Fig. 5. Mid-IR spectrum of the Crab Nebula . The spectrum features ionic forbidden lines superimposed onto a flat continuum synchrotron emission. The full line represents the spectrum of the synchrotron radiation with a spectral index of -0.5 after Douvion et al. (2001)

ISOPHOT at higher spatial resolution reveal that about half this excess is attributable to two peaks, separated by $\sim$ 80 arcsec (Green, Tuff, & Popescu 2004).

Spectro-imaging observations between 6.5 and 16.5 μm of the central 3 arcmin×3 arcmin part of the nebula at a spatial resolution of 6 arcsec were obtaind by Douvion et al. (2001) with ISOCAM . Ionic lines of [Ne II], [Ne III], [Ne V] at respectively 12.8, 15.5 and 14.3 μm, of [Ar II], [Ar III] at 7.0 and 9.0μm and of [S IV] at 10.5 μm were detected superimposed onto a flat continuum synchrotron emission (Figure 5). This confirms that the mid-IR emission from the Crab is dominated by synchrotron radiation; no dust is detected in this spectral region.

3. Spitzer Images

Images of the Crab Nebula at 3.6, 4.5, 5.8, 8.0, 24, and 70 μm were obtained with the *Spitzer Space Telescope* IRAC and MIPS cameras (Temim et al. 2006). Figure 6 reports the four IRAC images (panel c,d,e,and f) of the central part of the nebula. The pulsar, and

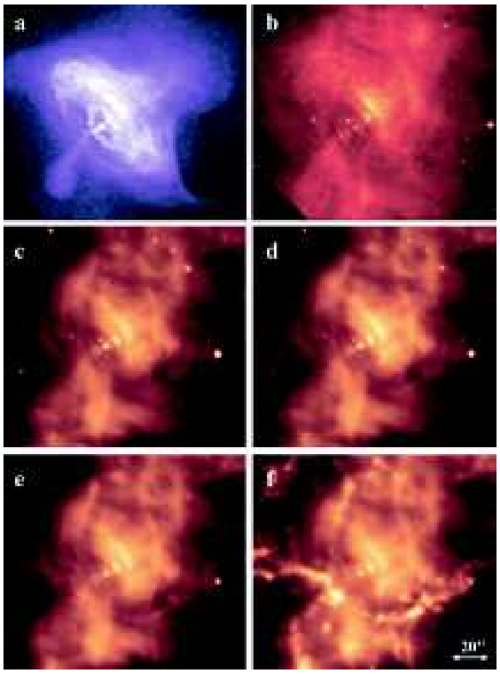

Fig. 6. *SPITZER/IRAC* images at 3.6, 4.5, 5.8 and 8.0 μm of the central part of the Crab Nebula. The *Chandra* X-ray ACIS-S and *HST* optical images are reproduced for comparison after Temim et al. (2006).

the associated equatorial toroid and polar jet structures seen in *Chandra* and *Hubble Space Telescope* images (panel a, and b in Fig.6) can be identified in all of the IRAC images. The 8.0 μm image, including the [Ar II] 7.0 μm line, resembles the general morphology of visible H_α and near-IR [Fe II] line emission, while the 3.6 and 4.5 μm images are dominated by continuum synchrotron emission.

4. H_2 molecular knots

H_2 emission at 2.12 μm was detected in two filaments of the Crab Nebula by Graham, Wright, & Longmore (1990). Although the measurements were made through a 19 arcsec diameter aperture, which averages over a large and complicated region in the filamentary structure at both locations, this discovery raises fashinating questions about the origin, survival, and excitation of the molecular gas in the Crab. Very recently sub-arcsec images centered on the H_2 line confirm the presence of these knots in the filaments of the nebula (Persi et al. 2011), (Loh, Baldwin, & Ferland 2010). Figure 7 reports the narrow-band images obtained at the TNG telescope with the NIR camera NICS.

A survey of molecular hydrogen in the whole Crab Nebula has been undertaken by Loh, et al. (2011) . The authors detected 55 knots that emit strongly in the H_2 line. The knots generally fall on or next to optically bright filaments. Comparison of the positions and structures of the H_2 knots to the morphology seen in HST optical-passband [S II] and [O III] images shows that most H_2 knots are associated with low-ionization (large I([S II])/I([O III]) gas.

Graham, Wright, & Longmore (1990) considered in some detail three possible methods for exciting the H_2 emission: UV fluorescence, shocks, and heating by fast electrons. High resolution spectroscopy in the K-band is necessary to understand the mechanisms of exciting the H_2 emission in the Crab.

5. Summary

In this paper the main infrared observations of the Crab Nebula are discussed. From these observations, the following conclusions can be derived:

a) The near and mid-IR continuum in the Crab Nebula is dominated by synchrotron emission. Ionic lines have been observed in these spectral regions with a filamentary structure similar to that observed in the optical lines.

b) A break in the spectral energy distribution between 60 and 100 μm suggests the presence of dust at a temperature of 46K and with mass of 0.02 M_{sun} .

c) The structures observed in the optical and X-ray associated with the pulsar are also present in the near-IR untill 8 μm.

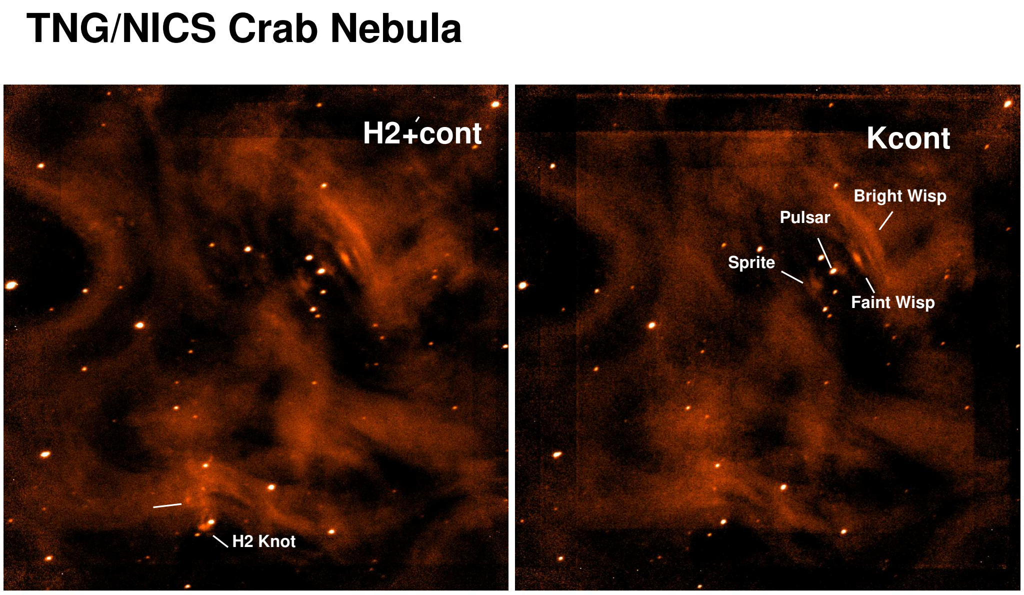

Fig. 7. H $_2$ and Kcont images of the Crab Nebula taken at the italian telescope TNG with the NIR camera NICS.

d) H_2 emission at 2.12 μm was found associated with the filaments of the Crab . Coordinated Xray(Chandra), optical (Hubble) and NIR observations are planned in order to understand the physical processes inside the Crab Nebula.

References

Becklin, E.E. & Kleinmann , D.E. 1968, ApJ, 152, L52

Douvion, T. et al. 2001, A&A, 373, 281

Graham, J.R., Wright, G.S., & Longmore , A..J. 1990, ApJ, 352, 172

Grasdalen, G.L. 1979, PASP, 91, 436

Green, D.A., Tuff, R.J., & Popescu , C..C. 2004, MNRAS, 355, 1315

Herster, J.J. et al. 1990, ApJ, 357, 539

Marsden, P.L. et al. 1984, ApJ, 278, L29

Melatos, A. et al. 2005, ApJ, 633, 931

Strom, R.G., & Greidanus , H. 1992, Nature, 358, 654

Loh, E.D., Baldwin, J.A., & Ferland , G.J. 2010, ApJ, 716, L9

Loh, E.D., et al. 2011, ApJS, 194, 30

Persi, P. et al. 2011, in preparation

Temim, T. et al. 2006, AJ, 132, 1610